

Injectorless quantum cascade lasers for room-temperature short-wavelength emission by efficient second-harmonic generation

Augustinas Vizbaras^{1*}, Simeon Katz¹, Matthias Anders¹, Christian Grasse¹, Gerhard Boehm¹, Ralf Meyer¹, Mikhail A. Belkin² and Markus-Christian Amann¹

¹ *Walter Schottky Institut, Technische Universität München, Am Coulombwall 3, 85748 Garching, Germany*

² *Department of Electrical and Computer Engineering, The University of Texas at Austin, Austin, TX 78758, USA*

* *E-mail: augustinas.vizbaras@wsi.tum.de*

1. Introduction

Semiconductor laser sources operating in the wavelength range from 2 μm to 15 μm are attractive components for numerous spectroscopy and free-space communication applications. However, wavelengths below 4 μm have been difficult to achieve due to limited conduction band offsets for the barrier materials and carrier scattering into indirect valleys of the well material [1]. A different approach to generate short wavelengths is to use intracavity frequency doubling. This has been successfully demonstrated in quantum cascade lasers [2]. However, their operation has been limited to cryogenic temperatures. Recently, a novel device design for nonlinear frequency mixing was proposed [3], which allows RT operation at wavelengths around 3.7 μm with peak output powers of around 150 nW at 14 kA/cm² [3]. For most applications, CW operation is often required, thus operating current densities have to be minimized, which is difficult to achieve without losing output performance. In this work we propose the use of strain-balanced injectorless QCL active regions for pumping the nonlinear section. Such injectorless QCLs have been shown to possess low threshold current densities and relatively high efficiencies [4, 5]. Here we demonstrate RT second-harmonic generation around 2.7 μm with peak output powers close to 10 μW at current densities of around 2 kA/cm². We will also discuss possible device structures for wavelengths around 3.5 μm and a future development strategy for single-mode, two-color tunable laser sources.

2. Device design and performance

Devices presented in this paper consist of a 1.5 μm (60 periods) thick strain-balanced injectorless QCL ($\lambda = 5.4 \mu\text{m}$) with an active region similar to the one reported in [5], followed by 55 periods of a 2-well nonlinear (NL) section (Fig. 1 (a)). This structure was grown by solid-source MBE. After growth, the wafer was patterned into lasers with different longitudinal NL filling factors (Fig. 1 (b)), and the non-patterned section of the NL layer was selectively removed. Afterwards, the sample surface was cleaned and transferred into MOVPE, where the top InP waveguide and GaInAs contact layers were overgrown. Finally, the devices were processed as deep-etched ridge-waveguide devices with different longitudinal filling factors of the NL layer F ($F = L_{\text{NL}}/L_{\text{ridge}}$), and cleaved into different lengths for characterization. The schematic device structure is shown in Fig. 1 (b).

Preliminary experimental data is shown Fig. 2. Here RT and 80 K second-harmonic (SH) L-I curves are shown in Fig. 2 (a) with a typical emission spectrum in Fig. 2 (b). We see that devices with $F = 30\%$ possess mW level SH peak output powers (around 1.2 mW) at 80 K (Fig. 2 (a)) with an extremely high power conversion efficiency around 100 mW/W^2 . However, the device does not operate at room temperature due to high additional losses introduced by the large F value. Therefore, for room-temperature operation, we used a device with only $F = 4\%$, which has negligible additional loss. This device was able to achieve $9.5 \text{ } \mu\text{W}$ peak power at $20 \text{ }^\circ\text{C}$ at $\lambda = 2.75 \text{ } \mu\text{m}$ with a peak conversion efficiency of 0.77 mW/W^2 .

In summary, these results are very encouraging and clearly show the potential of injectorless QCLs for efficient nonlinear frequency generation. This could become very important to achieve efficient RT operation at very short wavelengths or in the THz frequency range.

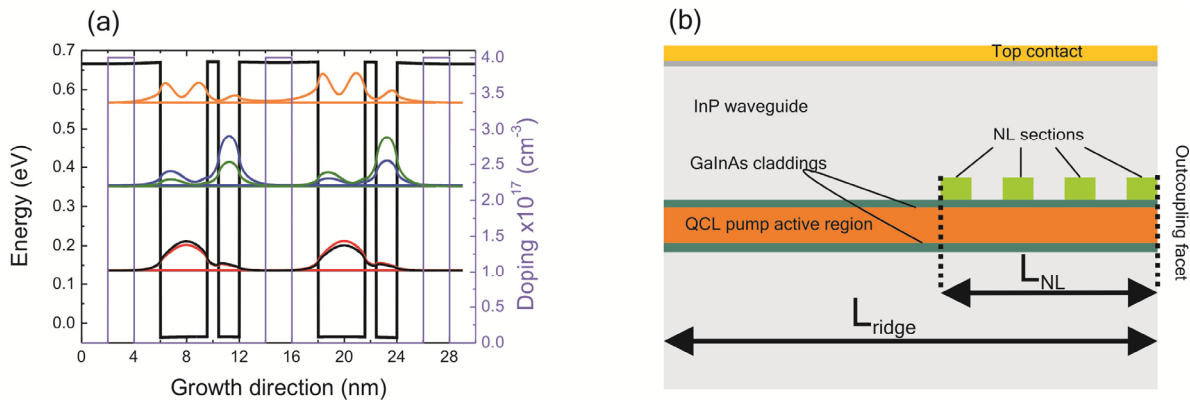


Fig. 1. (a) Conduction band diagram of two periods of the NL section. The layer sequence in nm is **6/3.57/0.85/1.59** where $\text{Al}_{0.55}\text{In}_{0.45}\text{As}$ barriers are shown in bold, and $\text{Ga}_{0.35}\text{In}_{0.65}\text{As}$ well in normal font. (b) Schematic drawing of our device.

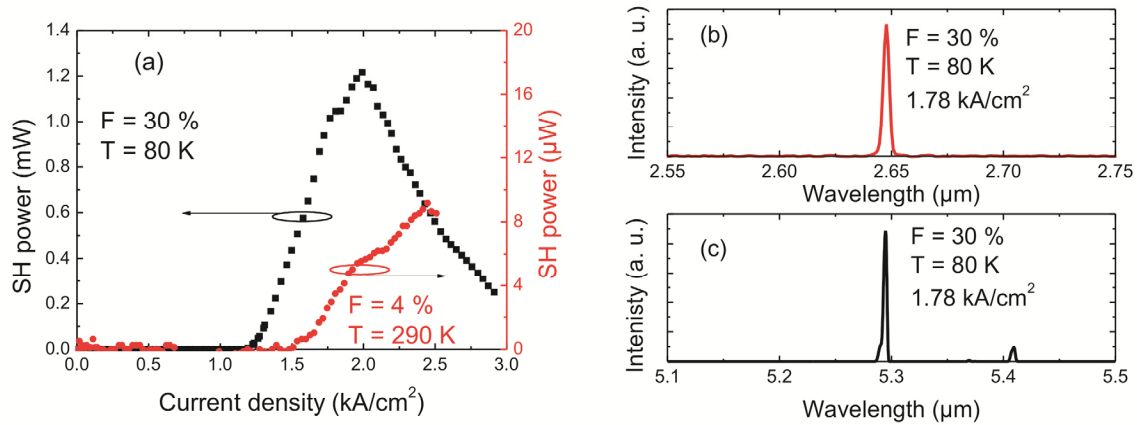


Fig. 2. (a) L-I curves for two best devices at 80 K and 290 K, and typical emission spectra of the (b) second-harmonic and (c) pump signals. The device with $F = 30\%$ was 3.5 mm long and $12 \text{ } \mu\text{m}$ wide, whereas the $F = 4\%$ device was 5 mm long and $12 \text{ } \mu\text{m}$ wide. NL sections in both devices were structured to serve as 1^{st} order quasi-phase matching gratings with a period of $37 \text{ } \mu\text{m}$.

3. References

- [1] O. Cathabard et al., Appl. Phys. Lett. **96**, 141110, (2010).
- [2] C. Gmachl et al., IEEE J. Quantum Electron., **39**, 1345-1355, (2003).
- [3] M. Jang et al. Proc. Of CLEO/QELS 2010, San Jose, USA (2010).
- [4] S. Katz et al. Electron. Lett. **44**, 580-581, (2008).
- [5] S. Katz et al. Appl. Phys. Lett. **94**, 151106, (2009).